Available online at www.sciencedirect.com
ScienceDirect
Journal of Catalysis 256 (2008) 1–14
JOURNAL OF CATALYSIS
www.elsevier.com/locate/jcat

Active sites of olefin metathesis on molybdena-alumina system: A periodic DFT study

Jarosław Handzlik [a], Philippe Sautet [b,*]

[a] *Institute of Organic Chemistry and Technology, Cracow University of Technology, ul. Warszawska 24, PL 31-155 Kraków, Poland*
[b] *Université de Lyon, Institut de Chimie de Lyon, Laboratoire de Chimie, École Normale Supérieure de Lyon and CNRS, 46 Allée d'Italie, 69364 Lyon Cedex 07, France*

Received 14 November 2007; revised 15 February 2008; accepted 15 February 2008

Available online 8 April 2008

Abstract

A periodic DFT approach was used to investigate ethene metathesis on a molybdena-alumina catalyst. Ten potential monomeric Mo-methylidene centers variously located on the (100) and (110) surfaces of γ-alumina were modeled. The Mo sites differed from one another in terms of geometry, the number and type of Mo–O–Al linkages, and the number of free Mo=O bonds. The thermodynamic stability of the Mo-methylidene species was compared over a wide range of temperatures, taking into account the hydration state of the surface. Depending on water vapor pressure, structures bonded differently to the surface are stable. Moreover, the Mo sites on (110) γ-alumina are more stable than their analogues located on the (100) face. The pathways of ethene metathesis proceeding on the Mo-methylidene centers also were studied. The various Mo species demonstrate varying activity. Most of the Mo-methylidene centers are reactive with ethene and form molybdacyclobutane complexes, which can exist as two coordination isomers with possible interconversion. In many cases, the molybdacyclobutane species are significantly more stable than the reactants. Thus, metallacycle opening to restore carbene and olefin is the rate-limiting step for ethene metathesis. The large majority of the Mo sites, although reactive with ethene, are blocked at the molybdacyclobutane step, and their catalytic reactivity is small at room temperature. Only a small minority of sites are catalytically active. It is concluded that the most active site is located on the (100) surface and is stable in dehydrated conditions. At higher temperatures, however, other Mo species can be active in olefin metathesis.

Keywords: Density functional theory; Ethene metathesis; Molybdena-alumina catalyst

1. Introduction

Supported metal oxide catalysts are applied in a number of large-scale industrial processes based on alkene metathesis [1,2]; for instance, molybdena-alumina catalysts are used in the Shell Higher Olefins Process (SHOP), in which cross-metathesis is a key step. A number of theoretical investigations of olefin metathesis [3–11] have confirmed the carbene mechanism for this process [12], involving metal-alkylidene complexes and metallacyclobutane intermediates. In the case of the supported molybdenum systems, surface Mo-alkylidene species are formed after contact with alkene or cycloalkane, after thermal pretreatment of the catalyst [2,13–15]. In contrast to well-defined catalytic systems of olefin metathesis, the structures of the surface alkylidene centers are not determined unambiguously. Identifying the active sites at a molecular level remains an important challenge in heterogeneous catalysis. In the case of the monomeric centers, which we consider in this paper, a tetrahedral site with one oxo ligand, one alkylidene ligand, and two oxygen linkages between the molybdenum atom and the support has been suggested [2,13,16,17]. Distorted tetrahedral dioxo Mo(VI) species or their reduced forms can be the precursors of these monomeric Mo-alkylidene sites [2,13,16–18]. Raman, EXAFS, and NEXAFS studies have confirmed tetrahedral coordination of the surface Mo(VI) oxide forms [19–22], which often are proposed to be dioxo species [19,21,22]. On the other hand, experimental evidence for the existence of monooxo surface monomeric Mo(VI) species under dehydrated conditions has been reported, based on Raman

* Corresponding author.
E-mail address: philippe.sautet@ens-lyon.fr (P. Sautet).

0021-9517/$ – see front matter
doi:10.1016/j.jcat.2008.02.016

and IR spectroscopy [23–27]. This species can be three- or four-coordinated to the surface [23,26,27], and analogous structures for the Mo-alkylidene centers could be expected as well. A dynamic method for chemical counting of active sites led to a recent assertion that the number of active sites is <1% of the total number of Mo atoms [28].

Concerning the structure of intermediates, it has been shown experimentally [29–32] that for the homogeneous Schrock catalysts Mo(NAr)(CHR)$(OR')_2$ and W(NAr)(CHR)$(OR')_2$, the metallacyclobutane intermediates have either a trigonal bipyramidal (TBP) geometry with a flat ring or a square pyramidal (SP) conformation with a puckered ring. Both the stability of the given metallacyclobutane type and the activity of the catalyst are governed by, among other factors, the electronic properties of the alkoxide ligands [3,4,29–32]. In the case of the supported catalysts, the carrier can be considered a multidentate ligand of the metal center [33,34]. Theoretical investigations of the molybdena-alumina system, using cluster models for the surface, showed that both the local electronic properties of the support and the geometry of the active sites affect the relative stability of the molybdacyclobutane complexes and the reactivity in alkene metathesis [10,11].

In the present work, a periodic slab model was used for the first time in a periodic DFT approach to study olefin metathesis on a molybdena-alumina system. In contrast to the cluster model, this approach avoids introducing edge effects and allows a better description of surface relaxation effects. Monomeric Mo-methylidene centers on alumina were modeled, applying the recently reported γ-alumina model [35–38]. Our main aim was to identify the geometry and location of a large family of potential Mo-methylidene species on the surface. The key questions are focused first on the probability of existence of these sites, related to their relative energy, and second on their respective metathesis activity. A central aspect of the investigation is determining whether all sites are similarly active or whether only a small fraction of them is responsible for the catalytic activity. Therefore, we compared the stability of various proposed structures of the active sites on both the (100) and (110) faces of γ-alumina, taking into account the hydration status of the surface. We also studied molybdacyclobutane intermediates, the products of the addition of ethene to the respective Mo-methylidene sites. For the most relevant cases, we calculated full pathways of ethene metathesis, to gain insight into the potential structures that dominate metathesis activity.

2. Computational methods and models

The periodic calculations were performed within the framework of density functional theory (DFT), using the Vienna Ab Initio Simulation Package (VASP) [39–41] and the Perdew and Wang (PW91) generalized gradient-corrected exchange-correlation functional [42]. A basis set of plane waves was used to represent the one-electron wave functions. Atomic cores were described with the projector-augmented wave method (PAW) [43]. A cutoff energy of 400 eV yielded a converged total energy. A 331 Monkhorst–Pack mesh was applied for Brillouin-zone sampling. Transition state structures have been localized using the nudged elastic band (NEB) method [44,45]. The stationary points were all converged with the quasi-Newton algorithm; in two test cases, they were characterized by a frequency calculation.

The models of the γ-Al_2O_3 surface, based on the earlier developed nonspinel bulk structure with a $5.59 \times 8.414 \times 8.097$ Å^3 box containing 8 Al_2O_3 units [46], were validated previously [35,36]. The (110) plane of γ-alumina is the most exposed surface on the particles (80%), and the (100) surface is in the minority (17%); the (111) plane can be neglected [35,47,48]. On the other hand, the calculated surface energy for dehydrated (100) γ-Al_2O_3 is lower than for dehydrated (110) γ-Al_2O_3 [35,36]. Both the (100) and (110) faces were taken into account in the present study. Surfaces were modeled by a four-layer slab, with the two bottom layers frozen in the calculated geometry of the bulk and the two upper layers relaxed. The surface unit cell dimensions were $a = 8.414$ and $b = 11.180$ Å for the former and $a = 8.097$ and $b = 8.414$ Å for the latter, corresponding to two and one unit cells used to describe the bulk structure of γ-alumina.

Mo-alkylidene sites in real catalysts are formed from the precursors at low or moderate temperatures under dehydrated conditions, with the catalyst pretreated in situ at high temperature, ca. 800–1100 K [14,15,28]. For the (100) surface of γ-alumina, a fully dehydrated surface is thermodynamically favored at such temperatures, whereas the coverage is 3.0–5.9 OH per nm^2 on the (110) surface, according to the periodic DFT and thermodynamic calculations with a vapor pressure of 1 atm assumed [35,36]. This coverage corresponds to 1 or 2 water molecules adsorbed per surface unit cell. Because the presence of the Mo site on the surface is approximately equivalent to adsorption of one or two water molecules (vide infra), and the actual metathesis process is carried out in dehydrated conditions, in most cases no water molecules have been added to the alumina surface containing the models of the Mo species.

The dehydrated (100) surface exhibits five-coordinated Al Lewis centers (Al_V), arising from octahedral Al in the bulk, with tetrahedral Al located below the surface plane. The dehydrated (110) surface demonstrates stronger Lewis acidity, along with Al_{IV} (from octahedral Al in the bulk) and Al_{III} centers (from tetrahedral Al in the bulk). These various unsaturated sites were used to attach the Mo-methylidene centers. All models considered a Mo atom at the +VI oxidation state.

To calculate the reaction and activation Gibbs free energy, we approximated the differences between the Gibbs free energies for condensed phases by the differences in their calculated electronic energies. Only the rotational and translational contributions to enthalpy and entropy of gas molecules (i.e., water, ethene) were taken into account; that is, we assume that the vibrational contribution of a gas molecule is not significantly influenced by its adsorption.

Surface deformation energies were calculated as the energy difference between the alumina part in the Mo/γ-Al_2O_3 geometry and the free alumina surface in its relaxed geometry,

$$E_{\mathrm{def\,Al}} = E_{\mathrm{Al}}(\mathrm{frozen}) - E_{\mathrm{Al}}(\mathrm{relaxed}).$$

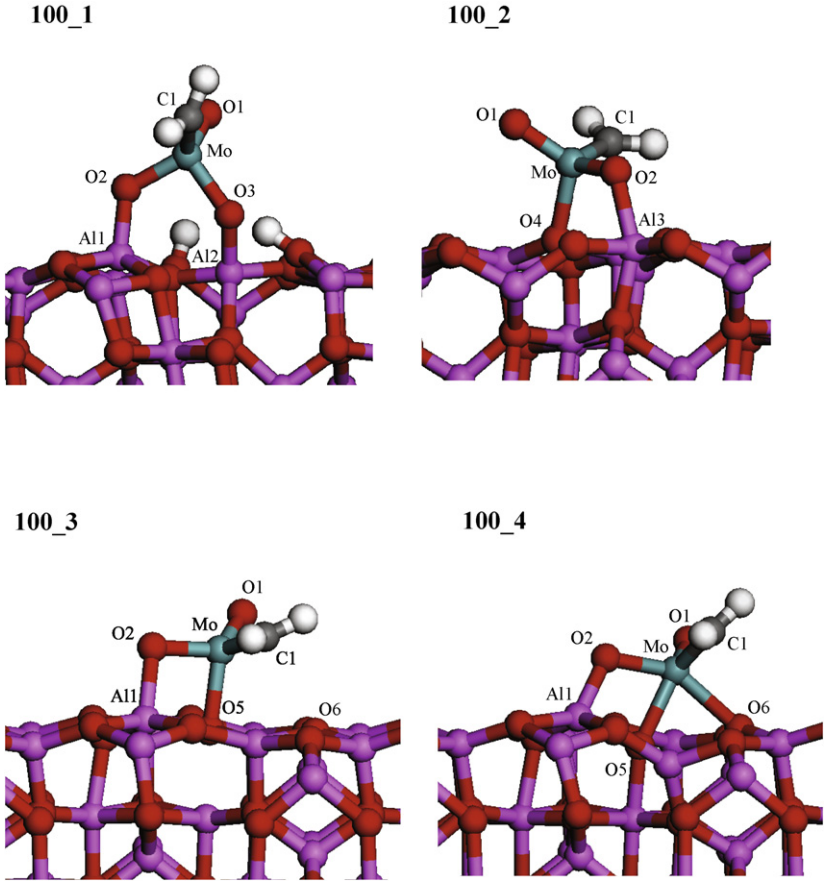

Fig. 1. Mo-methylidene centers on (100) γ-alumina.

Deformation energies for the anchored Mo species have been calculated in a similar way,

$$E_{\text{def Mo}} = E_{\text{Mo}}(\text{frozen}) - E_{\text{Mo}}(\text{relaxed}).$$

Interaction energies are defined as the difference between the energy of the whole system and the energies of the respective fragments in the Mo/γ-Al_2O_3 geometry,

$$E_{\text{int}} = E_{\text{system}} - E_{\text{Al}}(\text{frozen}) - E_{\text{Mo}}(\text{frozen}),$$

whereas adsorption energies are calculated as

$$E_{\text{ads}} = E_{\text{system}} - E_{\text{Al}}(\text{relaxed}) - E_{\text{Mo}}(\text{relaxed}).$$

3. Results and discussion

3.1. Mo-methylidene centers on (100) γ-alumina

Fig. 1 shows the models considered for the Mo-methylidene species on the (100) γ-Al_2O_3. In the first case (**100_1**), the molybdenum atom is connected via two oxygen linkages with octahedrally coordinated Al atoms (previously Al_V on the bare surface) and has one oxo ligand and the methylidene group. Such four-coordinate Mo-alkylidene surface complexes have been proposed to be the active metathesis sites [2,10,11,13,16,17]. The species **100_1** can be formally described as the product of the addition of the hypothetical Mo-methylidene complex $Mo(=O)(=CH_2)(OH)_2$ on the bare surface. Thus, along with the Mo complex, two hydrogen atoms were added to the clean surface of (100) alumina for stoichiometric reasons.

Table 1
Selected bond lengths (Å) and angles (°) for the Mo-methylidene centers on (100) γ-alumina

	100_1	100_2	100_3	100_4
Mo–C1	1.91	1.93	1.92	1.91
Mo–O1	1.72	1.72	1.72	1.71
Mo–O2	1.84	1.79	1.82	1.92
Mo–O3	1.93	–	–	–
Mo–O4	–	2.02	–	–
Mo–O5	–	–	2.06	2.21
Mo–O6	–	–	3.23	2.27
Al1–O2	1.80	–	1.92	1.80
Al2–O3	1.78	–	–	–
Al3–O2	–	1.99	–	–
O2–Mo–O3[a]	97	99	86	–
O2–Mo–C1	112	111	108	101

[a] O4 and O5 for the **100_2** and **100_3**, respectively.

Selected bond lengths and angles for the optimized geometry of **100_1** are given in Table 1. The predicted length of the carbene bond is close to the value reported for a homogeneous Mo-alkylidene system (1.88 Å) [29] and consistent with the results of previous cluster calculations [10,11]. The Mo–O1 distance is typical for the Mo=O double bond [49]. The differing lengths of the Mo–O2 and Mo–O3 single bonds (Table 1) results from the formation of a strong hydrogen bond between

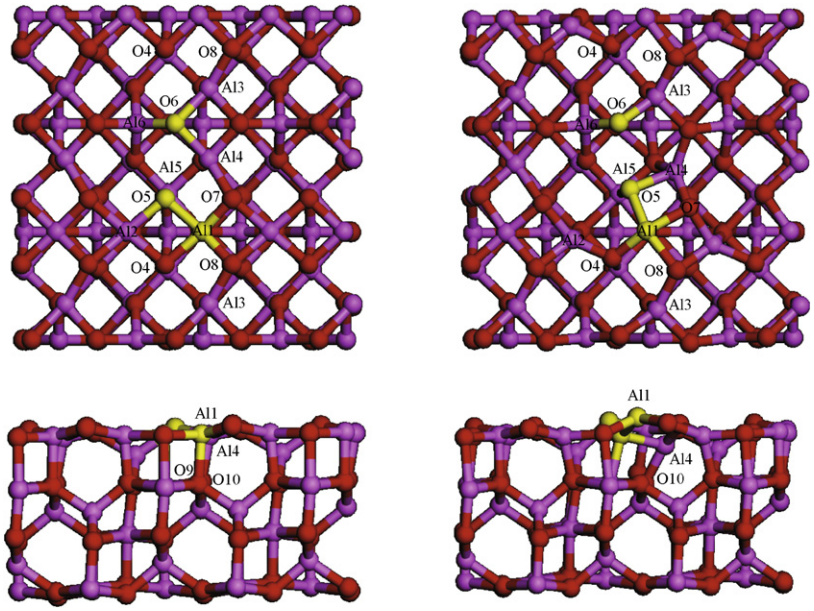

Fig. 2. Deformation of the γ-alumina (100) surface upon grafting of the **100_4** Mo center. Initial bare surface (left) and reorganized substrate for the **100_4** site (right). For clarity, the Mo site is removed, while the strongly affected Al1, O5 and O6 atoms are shown in yellow (or light grey).

the O3 atom and the surface hydrogen, as indicated by the short O3–H distance (1.49 Å).

The next two Mo-methylidene species considered (**100_2** and **100_3**, Fig. 1) have very similar geometries despite their different locations on the surface. They can be considered as the products of the addition of the hypothetical $Mo(=O)_2(=CH_2)$ unit on the surface, with one Mo=O bond bridging an (Al, O) pair. In these sites, the pseudotetrahedrally coordinated molybdenum is connected through only one oxygen bridge to a distorted octahedral aluminum atom. In addition, a weak dative bond is formed between the threefold-coordinated surface oxygen (O4 in **100_2** and O5 in **100_3**) and the metal center. For both structures, the Mo–O2 distance is shorter than in the case of **100_1,** and this bond actually seems to be intermediate between single and double (see Table 1). Consequently, the Al–O2 distance (1.99 and 1.92 Å) is elongated compared with **100_1**. Another common feature of both centers is the excellent exposure of the carbene bond toward an approaching alkene molecule.

The last Mo-methylidene structure on the (100) face of γ-alumina that we studied, **100_4,** is located similarly to the center **100_3** (Fig. 1), but with an additional dative bond formed between the molybdenum and the surface oxygen atom O6. It is not surprising that, according to the calculated distances, all other bonds with the surface are weakened compared with **100_3** and **100_2** (Table 1). In accordance with the bond order conservation principle, the Al1–O2 distance in **100_4** is shorter than that in **100_3** and **100_2** (Al3–O2 in this case).

It should be noted that the structures **100_2**, **100_3**, and **100_4** are isomers and that each can be considered the product of the dehydration of structure **100_1** (vide infra).

The presence of Mo species causes a significant deformation of the surface in their vicinity. As an example of this effect, Fig. 2 compares the clean (100) surface of γ-alumina with the surface modified by the **100_4** center. Table 2 gives the most relevant atomic distances. It can be seen that the Al1 atom, where the molybdenum is attached via the oxygen linkage, is shifted above the surface on formation of the Al1–O2 bond. Indeed, the bond trans to the new Al1–O2 bond (Al1–O9) is practically broken, as demonstrated by comparing the respective values in Table 2. In addition, the O5 atom on the modified surface is no longer coordinated to the aluminum Al2, but instead forms a new bond to the Al4 atom, which in turn is decoordinated from O6, improving its capability of interacting with the Mo atom. Thus, through a successive and cyclic redistribution of the Al–O bond strengths, the surface can adapt itself to the grafting of the complex and is not a static substrate. Together with the formation of the three bonds between the complex and the surface, three bonds are broken within the surface, while one bond is strengthened. This capability of the surface to rearrange its bonding pairs is a key feature for its strong interaction with the complex and is an advantage over such compounds as silica, in which such electronic redistribution is much more difficult.

Table 2
Atomic distances (Å) for the clean and modified by the **100_4** center (100) γ-alumina surface

	Clean surface	Modified surface
Al1–O4	1.85	1.83
Al1–O5	1.85	1.93
Al1–O7	1.84	1.95
Al1–O8	1.83	1.98
Al1–O9	1.91	2.67
Al2–O5	2.00	3.03
Al3–O6	1.91	1.82
Al4–O5	2.28	1.94
Al4–O6	1.91	3.05
Al4–O10	1.80	1.77
Al5–O5	2.01	1.99
Al6–O6	1.85	1.82

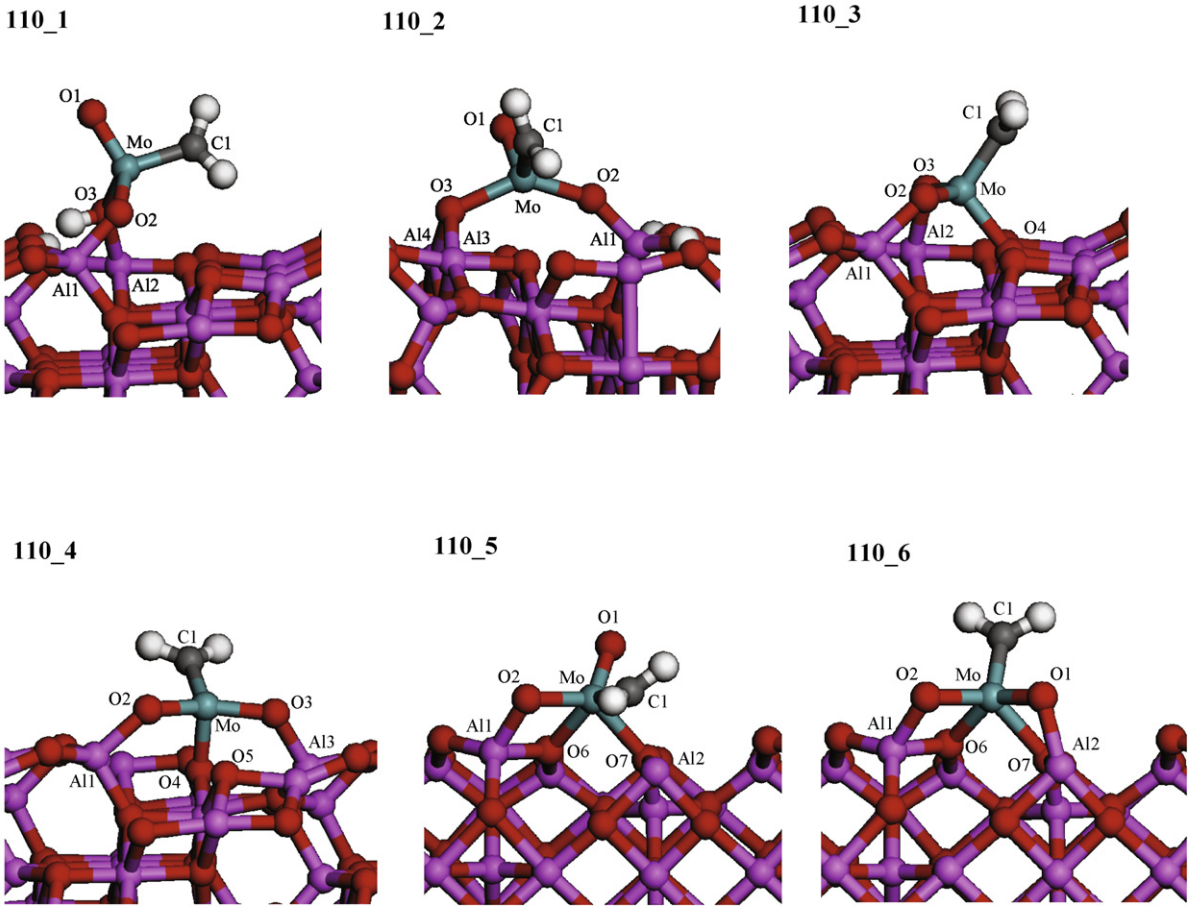

Fig. 3. Mo-methylidene centers on (110) γ-alumina.

Table 3
Selected bond lengths (Å) for the Mo-methylidene centers on (110) γ-alumina

	110_1	**110_2**	**110_3**	**110_4**	**110_5**	**110_6**
Mo–C1	1.89	1.90	1.89	1.90	1.95	1.89
Mo–O1	1.71	1.70	–	–	1.71	1.80
Mo–O2	1.86	1.90	1.80	1.82	1.88	1.85
Mo–O3	2.04	2.07	1.76	1.84	–	–
Mo–O4	–	–	2.04	1.89	–	–
Mo–O5	–	–	–	2.72	–	–
Mo–O6	–	–	–	–	2.11	2.05
Mo–O7	–	–	–	–	2.16	2.21
Al1–O2	1.77	1.71	1.85	1.87	1.80	1.82
Al2–O1	–	–	–	–	–	1.87
Al2–O3	1.86	–	1.96	–	–	–
Al3–O3	–	1.84	–	1.89	–	–
Al4–O3	–	1.85	–	–	–	–
Al2–C1	–	–	–	–	2.22	–

3.2. Mo-methylidene centers on (110) γ-alumina

Mo-methylidene species on the (110) surface are shown in Fig. 3, and their geometrical parameters are given in Table 3. In all but one case, the carbene bond is shorter compared with the Mo structures on the (100) γ-Al_2O_3 face.

The first model of the active site (**110_1**) presents a fourfold-coordinated Mo center analogous to the structure of **100_1**, with two aluminoxi linkages and one free carbene and oxo ligands. However, the molybdenum is connected with one tetrahedrally coordinated aluminum atom (Al1) and one octahedrally coordinated aluminum atom (Al2) instead of two octahedral Al atoms for the (100) surface. The single Mo–O3 bond is significantly elongated, because in this case the surface hydrogen atom prefers to bond to O3. The Mo center **110_1** also has been reoptimized after dissociative adsorption of one water molecule per Mo-methylidene complex on the surface, resulting in formation of a bridge hydroxyl group. The general structure of the active site remains intact, although with several minor changes in the geometric parameters. Because the metathesis reaction is carried out in dehydrated conditions (see Section 2), we did not examine this structure in ethene metathesis.

Through a combination of experimental study and DFT calculations, it was shown that terminal OH groups on the (110) γ-alumina are most reactive toward an incoming metal complex [50]. The grafting reaction involving the replacement of bridge OH groups also is possible. Therefore, we attempted to locate the Mo center in place of one terminal and one bridge hydroxyl. In the resulting structure (**110_2**; Fig. 3) the molybdenum has a distorted tetrahedral coordination and is connected via two oxygen atoms with one tetrahedrally coordinated aluminum atom (Al1) and two octahedrally coordinated aluminum atoms (Al3 and Al4); again, the single Mo–O3 bond is longer, because O3 is a bridge oxygen.

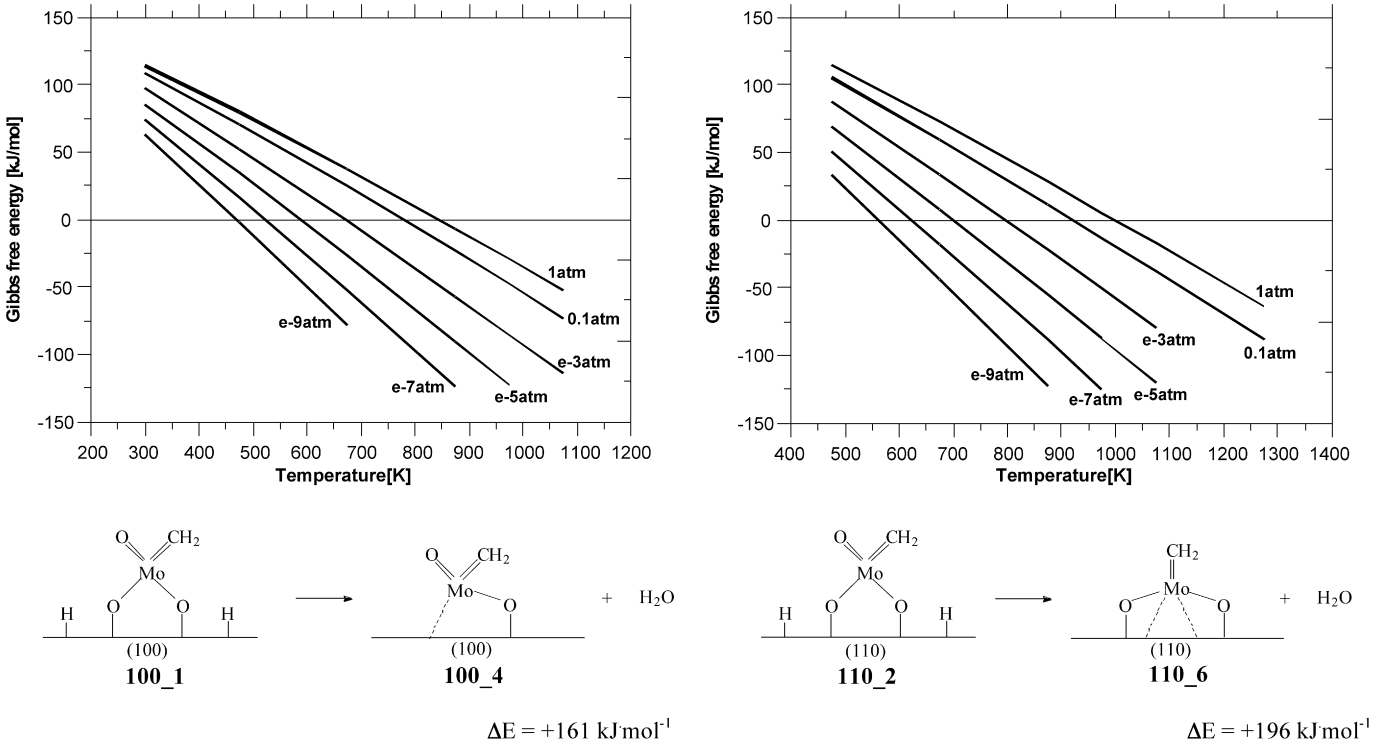

Fig. 4. Relative stabilities of the Mo-methylidene species as a function of temperature for different water vapor pressures.

The two Mo-methylidene species **110_3** and **110_4** (Fig. 3) are different than those described earlier. The molybdenum is still four-coordinated but has no free oxo ligand; instead, it is threefold-bonded to the surface. In **110_3**, the Mo atom is connected via two oxygen linkages with tetrahedrally (Al1) and octahedrally (Al2) coordinated aluminum atoms (the same atoms as in the **110_1** model) and interacts with a three-coordinated oxygen atom (O4) from the support. This structure can be viewed as a $Mo(=O)_2(=CH_2)$ unit distorted by interaction with the surface. The Mo–O2 and Mo–O3 bonds are elongated only slightly after interaction with the Al1 and Al2 on the surface and retain a partial double-bond character. The structure resembles **100_2**, but with both oxo groups interacting with the surface. The third Mo–O4 is a relatively weak dative bond from an oxygen lone pair on the surface, toward the Mo Lewis acid center.

Model **110_4** is quite similar to **110_3**, but with a different choice of octahedral Al atom on the surface (with Al2 replaced by Al3) for one aluminoxi linkage. This results in a strong reorganization of the surface, with breaking of the Al3–O4 bond (with both Al3 and O4 involved in the interaction with the grafted species) and strengthening of the Mo–O4 bond. Although the plane of the carbene bond is well exposed in both structures, the geometry of **110_4** is more favorable for alkene attack.

In the **110_5** structure (Fig. 3), the molybdenum atom shows an oxygen linkage with the tetrahedral Al1 atom, as in the other structures, but with two additional dative Mo–O bonds from two bridge surface oxygen atoms, O6 and O7. Similar weak Mo–O bonds are present in bulk MoO_3 [49]. On the other hand, the carbene bond is weakened in **110_5**, due to additional interaction between C1 and the surface aluminum Al2 (Table 3).

Finally, the Mo-methylidene center **110_6** (Fig. 3) is the only one in which the molybdenum is fourfold-bonded to the alumina surface. The complex initially was placed in exactly the same way as **110_5**, but with the methylidene group and the oxo ligand exchanged, resulting in formation of the O1–Al2 bond. Therefore, this molybdenum complex shows a distorted square pyramidal geometry with two single and two dative Mo–O bonds, along with the methylidene ligand on top. Similar to the Mo sites on (100) γ-alumina, the Mo-methylidene species **110_3**–**110_6** can be considered as the products of dehydration of the structures **110_1** and **110_2**.

3.3. Relative stabilities of the Mo-methylidene centers

The energies of the surface Mo complexes of identical stoichiometry can be directly compared with one another. Among the centers **100_2**, **100_3**, and **100_4** (Fig. 1), the latter is predicted to be the most stable. The energies of **100_2** and **100_3** are higher than that of **100_4** by 23 and 17 kJ mol^{-1}, respectively. As for the Mo-methylidene sites on the (110) γ-alumina (Fig. 3), **110_2** has a lower energy than **110_1** (by 71 kJ mol^{-1}), whereas **110_6** is the most stable species among the remaining Mo centers. The **110_3**, **110_4**, and **110_5** structures have higher energy than **110_6** (by 61, 76, and 42 kJ mol^{-1}, respectively).

When studying the relative thermodynamic stability of the Mo species, adequate dehydration reactions can be analyzed. For instance, the left-side reaction presented in Fig. 4 enables the calculation of the relative stabilities of the **100_1** and **100_4** sites. As can be seen, it is predicted that the former will be more stable than the latter at 0 K. An analogous situation is seen in

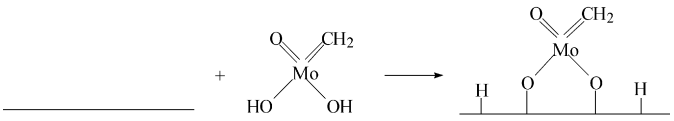

Scheme 1.

the Mo complexes on the (110) face, where the Mo-methylidene center **110_2** is thermodynamically preferred over the **110_6** one (Fig. 4, right-side reaction). However the situation changes when the temperature increases, due to the entropic effect of the released water molecules. In both reactions, the change of the Gibbs free energy at various temperatures and under various water vapor pressures was calculated (Fig. 4). The calculations indicate that at a water vapor pressure of 1 atm, the **100_4** site becomes more stable than the **100_1** site at temperatures above approximately 850 K. This threshold temperature decreases as the water vapor pressure is reduced; under low-pressure conditions, the "dehydrated" site can be more stable than the "hydrated" site at temperatures above approximately 500 K. As for the (110) surface, at a water vapor pressure of 1 atm, the thermodynamic preference for the "hydrated" complex **110_2** is observed up to approximately 1000 K, whereas under strict dehydrated conditions, the "dehydrated" site **110_6** can be more stable at temperatures as low as 600 K or higher.

The threshold temperatures in the dehydrated conditions are lower than those usually applied for the catalyst pretreatment step [14,15,28]. If the structures and relative stabilities of the isolated Mo(VI) oxide forms are similar to those of the Mo-methylidene centers, then the Mo(VI) oxide species analogous to the "dehydrated" Mo-methylidene centers should be present in the catalyst. But taking into account that the metathesis active sites are often formed from reduced Mo forms [14–16], determining whether the "dehydrated" Mo-methylidene centers are present during the reaction carried out at low temperatures is difficult.

The relative stabilities of the corresponding Mo forms on the (100) and (110) surfaces can be determined on the basis of the calculated energy for grafting the hypothetical Mo-methylidene complex $Mo(=O)(=CH_2)(OH)_2$ to the alumina (Scheme 1). The obtained reaction energy is -169 kJ mol^{-1} for the **100_1** center and -426 kJ mol^{-1} for the **110_2** center; therefore, the latter is predicted to be more stable than the former. This can be explained by the more unsaturated nature of the (110) surface with low-coordinated aluminum sites and strong Lewis acidity. These two quantities can be compared with the adsorption energy for two water molecules on the clean alumina surface. The calculated values are -176 kJ mol^{-1} for the (100) face and -425 kJ mol^{-1} for the (110) face. Thus, the adsorption of the Mo complex on the alumina is energetically equivalent to the adsorption of two water molecules.

Based on the energies obtained for the reactions depicted in Scheme 2, it can be seen that the center **100_4** has a less-stabilizing formation energy than the **110_6** one. Therefore, the present calculations indicate that the Mo-methylidene species on the (110) alumina are more stable than the corresponding ones on the (100) surface.

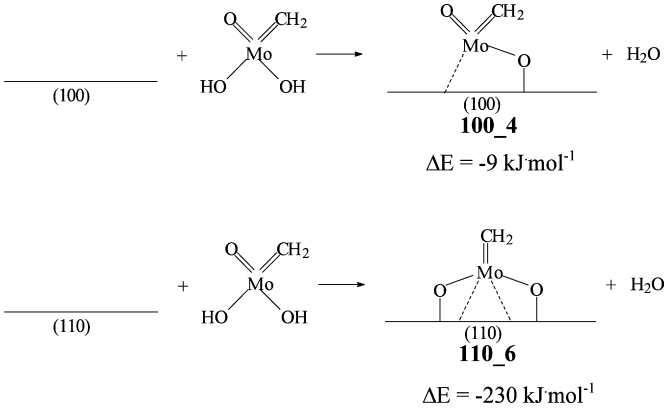

Scheme 2.

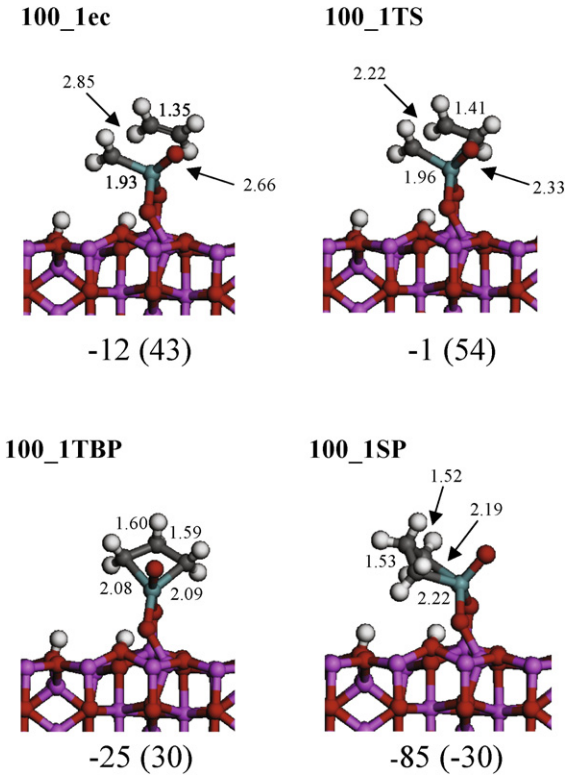

Fig. 5. Intermediates and transition states involved in ethene metathesis on the Mo-methylidene center **100_1**. The energies (kJ mol^{-1}) and Gibbs free energies (in parentheses, $T = 298$ K, kJ mol^{-1}), related to the reactants, are given below the structures.

3.4. Ethene metathesis: Mo sites on (100) γ-alumina

During the catalytic cycle of alkene metathesis, a metallacyclobutane intermediate is formed after a cycloaddition of alkene and a metal-alkylidene complex, followed by the cycloreversal step leading to the new alkene and another metal-alkylidene compound. To predict the activity of the proposed Mo-methylidene centers, we analyzed the possible conformations for the respective molybdacyclobutanes and, in selected cases, investigated the entire pathways of degenerate ethene metathesis.

The approach of an ethene molecule to the Mo-methylidene center **100_1** (Fig. 1) initially results in the formation of a weak

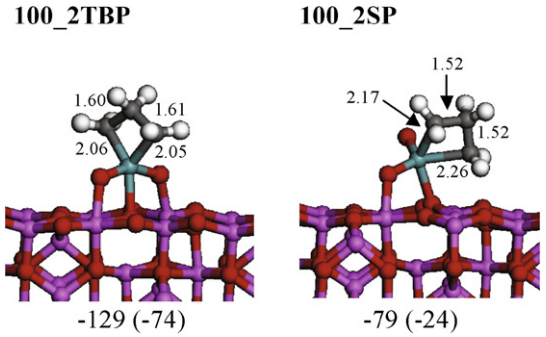

Fig. 6. Molybdacyclobutanes involved in ethene metathesis on the Mo-methylidene center **100_2**. The energies (kJ mol^{-1}) and Gibbs free energies (in parentheses, $T = 298$ K, kJ mol^{-1}), related to the reactants, are given below the structures.

ethene–molybdenamethylidene complex (**100_1ec**, Fig. 5). The predicted activation energy of its further conversion to the molybdacyclobutane intermediate **100_1TBP** is very low, about 11 kJ mol^{-1}. This initial molybdacyclobutane complex has a trigonal bipyramidal (TBP) geometry and can rearrange to the isomeric structure **100_1SP** with a square pyramidal (SP) geometry of the metal complex. This step is expected to proceed rather easily [10,11]. The existence of both types of molybdacyclobutane complexes has been experimentally [29–32] and theoretically [3–5,9] confirmed for the homogeneous Schrock systems and also has been predicted for the molybdena-alumina metathesis catalyst based on cluster calculations [10,11]. The calculated Mo–C distances in the SP structure (Fig. 5) are close to the experimental bond lengths obtained for this class of molybdacyclobutanes [30]. The geometrical parameters for the TBP and SP intermediates, as well as for the transition state, also are consistent with earlier theoretical results [10,11].

The formation of the TBP intermediate from the Mo-methylidene center **100_1** and ethene is only moderately exothermic ($\Delta E = -25$ kJ/mol). The further step in the metathesis mechanism—opening the molybdacyclobutane—is here just the reverse reaction for our degenerate ethene metathesis model. Thus, it is moderately endothermic, and its activation energy is reasonable (24 kJ mol^{-1}). Consequently, high metathesis activity for the **100_1** center would be predicted. However, the transformation of the TBP molybdacyclobutane to the SP isomer is predicted to be highly exothermic (by 60 kJ mol^{-1}), in agreement with the earlier cluster calculations for this system [10]. The estimated Gibbs free energy of **100_1SP**, related to the Mo-methylidene + ethene, is clearly negative (−30 kJ mol^{-1}) at 298 K. Once the SP isomer is formed, the metallacycle opening becomes strongly endothermic and activated (barrier, 84 kJ mol^{-1}); thus, this species accumulates on the surface at low temperature, resulting in poor metathesis catalytic activity. If the temperature is increased, the free energy difference is reduced (−14 kJ mol^{-1} at 373 K and 9 kJ mol^{-1} at 473 K) due to an entropic loss of adsorbing ethene; however, the activation barrier should remain high.

The reaction of ethene with the Mo-methylidene center **100_2** results in formation of the molybdacyclobutane **100_2TBP** (Fig. 6). In this case, significant reconstruction of the Mo center is observed. The initially terminal oxo lig-

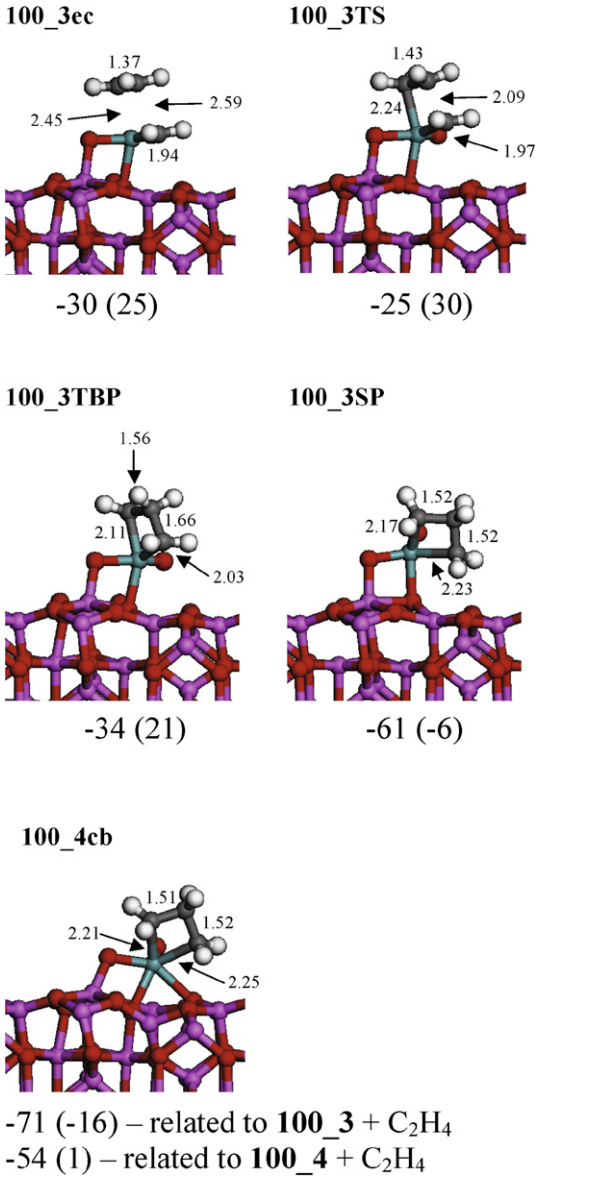

Fig. 7. Intermediates and transition states involved in ethene metathesis on the Mo-methylidene center **100_3** and **100_4**. The energies (kJ mol^{-1}) and Gibbs free energies (in parentheses, $T = 298$ K, kJ mol^{-1}), related to the reactants, are given below the structures.

and O1 becomes bonded to a surface aluminum in the final molybdacyclobutane structure. The reaction is predicted to be highly exothermic and irreversible, because the predicted Gibbs free energy is −74 kJ mol^{-1} at 298 K and −35 kJ mol^{-1} at 473 K. Consequently, this intermediate is even more stable (by 50 kJ mol^{-1}) than the corresponding square-pyramidal molybdacyclobutane, in which the free oxo ligand is again recovered (Fig. 6). Thus, the Mo-methylidene center **100_2** does not seem to be a suitable model of the metathesis active site, because of excessive stability of the molybdacyclobutane intermediate; indeed, the energy barrier for the metallacycle opening would be higher than 74 kJ mol^{-1}.

Although the geometry of **100_3** is very similar to that of **100_2** (Fig. 1), their reactivity differs significantly, according to our calculations. The formation of the first molybdacyclobu-

tane product (**100_3TBP**, Fig. 7) from **100_3** and ethene is moderately exothermic (with a small positive Gibbs free energy change at 298 K) and involves a very low activation barrier (5 kJ mol^{-1}). Therefore, this structure is predicted to be a reactive intermediate, easily splitting backward into the Mo-methylidene site and ethene, in contrast to the situation for **100_2TBP.** The key difference is that **100_3TBP** cannot be further stabilized by an additional oxo-Al interaction as **100_2TBP** can. At an early stage of ethene addition to **100_3**, the ethene-molybdenamethylidene complex **100_3ec** is formed. Its stability is close to that of **100_3TBP**. The square-pyramidal molybdacyclobutane **100_3SP**, which is of lower energy than the TBP isomer (by 27 kJ mol^{-1}), also has been localized. The former is predicted to be in thermodynamic equilibrium with the reactants (i.e., Mo-methylidene + ethene [$\Delta G = -6$ kJ mol^{-1} at 298 K]). Based on its relative energy (Fig. 7), we can conclude that reverse isomerization to the TBP intermediate followed by the cycloreversal step is possible even at low temperatures. The overall calculated barrier for the metallacycle opening from **100_3SP** is 36 kJ mol^{-1}; therefore, the Mo-methylidene species **100_3** seems to be a good candidate for the active site of olefin metathesis.

From Tables 1 and 4, changes in selected geometrical parameters along the reaction pathway on (100) γ-alumina can be seen. In most cases, the formation of the TBP intermediates via the TS structures involves elongation of the single Mo–O bonds compared with the corresponding Mo-methylidene sites. Exceptions are the Mo–O2 bond for the **100_2** series and the Mo–O3 bond for the **100_1** series. In the latter case, however, the Mo–O3 distance is increased in the TS structure. Further formation of the SP molybdacyclobutanes almost restores the initial values of the Mo–O bond lengths; this also holds true for the O2–Mo–O3 angle, whereas its value is clearly decreased in the TS and TBP structures.

Due to its rigidity, the surface imposes constraints on the geometry of the Mo centers. We compared the surface metallacycle species with an ideal gas-phase system Mo(=O)(C_3H_6)-$(OH)_2$, in which the OH model ligands are completely free (Table 4). It is striking to see that the quantities considered for **100_1TBP** are very close to those for the ideal **TBP** system. The calculated energy of **TBP** formation (−33 kJ mol^{-1}) is also not far from the respective value for **100_1TBP** (−25 kJ mol^{-1}), although, rather fortuitously, excellent consistency is observed with the **100_3TBP** structure (−34 kJ mol^{-1}). It should be noted, however, that not only geometrical constraints, but also the local electronic properties of the support influence the relative stability of the TBP molybdacyclobutanes [10,11]. Nevertheless, the most relevant species for metathesis reactivity are the SP metallacycles. Among these SP surface sites, the geometry of **100_1SP** is most similar to that of the ideal gas-phase model structure **SP**, whereas the geometries of the other SP centers differ more significantly (e.g., elongated Mo–O3, reduced O2–Mo–O3 bite angle). The energy of gas-phase model **SP** (−96 kJ mol^{-1}), related to the reactants (Mo-methylidene + ethene), is also closest to the relative energy of the **100_1SP** molybdacyclobutane (−85 kJ mol^{-1}).

Table 4
Selected bond lengths (Å) and angles (°) for the molybdacyclobutanes and transition states on (100) γ-alumina. A comparison with ideal gas systems Mo(=O)(C_3H_6)$(OH)_2$

System	Mo–O2	Mo–O3[a]	O2–Mo–O3[a]	O2–Mo–C[b]
100_1TS	1.89	1.98	87	107; 77
100_1TBP	1.93	1.93	87	90; 85
100_1SP	1.85	1.94	95	137; 90
100_2TBP	1.79	2.14	77	98; 101
100_2SP	1.80	2.08	91	134; 97
100_3TS	1.89	2.15	78	110; 83
100_3TBP	1.90	2.15	77	107; 84
100_3SP	1.84	2.04	85	132; 93
TBP (ideal)	1.95	1.93	89	83; 89
SP (ideal)	1.91	1.91	108	136; 83

[a] O4 and O5 for the **100_2** and **100_3** series, respectively.
[b] For each pair, the first value corresponds to the O2–Mo–C1 angle.

Table 5
Deformation energies of the Mo(=O)$_2$(C_3H_6) fragment ($E_{\text{def Mo}}$) and alumina surface ($E_{\text{def Al}}$), as well as the interaction (E_{int}) and adsorption (E_{ads}) energies (kJ mol^{-1})

	100_2SP	**100_3SP**
$E_{\text{def Mo}}$	135	149
$E_{\text{def Al}}$	122	218
E_{int}	−295	−393
E_{ads}	−38	−26

Among the SP molybdacyclobutane species considered on (100) γ-alumina, **100_3SP** is the least stable at −61 kJ mol^{-1} (35 kJ mol^{-1} less stable than the gas-phase model). This is the key point explaining its high reactivity. Its energy is higher than that of the very similar structure **100_2SP**, by 12 kJ mol^{-1}. To explain this difference, we decomposed the energy of both systems into the energy to distort the molecule part Mo(=O)$_2$(C_3H_6), the energy to distort the surface, and the interaction energy between the distorted entities (Table 5). The deformation energies are clearly higher for **100_3SP** (especially the alumina surface) than for **100_2SP**. This energy loss is not entirely balanced by the gain in the interaction energy, and thus the center **100_3SP** is less stable than **100_2SP**, as can be seen by comparing the respective adsorption energies. Thus, the constraint imposed by the rigid alumina surface and the energy cost of its deformation are the key factors in the creation of Mo centers resulting in a moderate stabilization of the SP metallacycle and hence high reactivity.

Among the species **100_2**, **100_3**, and **100_4** (Fig. 1), the latter is most stable; however, the energy differences are not large (see Section 3.3). According to our calculations, the cycloaddition of ethene on **100_4** leads to the same molybdacyclobutane as in the case of the Mo-methylidene center **100_3**; that is, **100_3TBP** is obtained. Therefore, breaking of the Mo–O6 bond is required for formation of the molybdacyclobutane product, and the species **100_4** can be considered a less active conformation of **100_3**. We also have found a molybdacyclobutane conformation with a puckered ring and distorted pentagonal pyramidal geometry (**100_4cb**, Fig. 7). Its formation from the Mo-methylidene complex **100_4** and ethene is

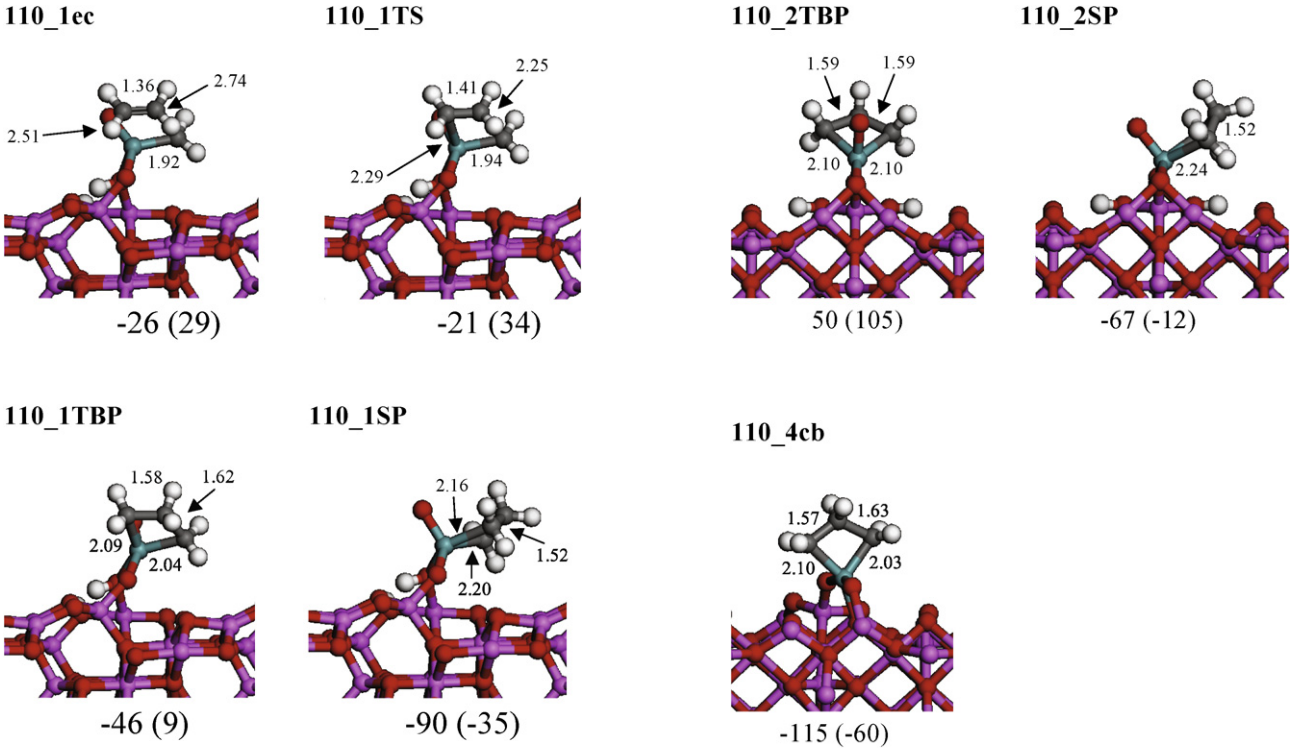

Fig. 8. Intermediates and transition states involved in ethene metathesis on the Mo-methylidene center **110_1**. The energies (kJ mol^{-1}) and Gibbs free energies (in parentheses, $T = 298$ K, kJ mol^{-1}), related to the reactants, are given below the structures.

Fig. 9. Molybdacyclobutanes involved in ethene metathesis on the Mo-methylidene centers **110_2** (**110_2TBP**, **110_2SP**) and **110_4** (**110_4cb**). The energies (kJ mol^{-1}) and Gibbs free energies (in parentheses, $T = 298$ K, kJ mol^{-1}), related to the reactants, are given below the structures.

slightly less exothermic than the formation of **100_3SP** from **100_3** and ethene. But **100_4cb** has lower energy than **100_3SP** (by approximately 10 kJ mol^{-1}), and if formed, actually may be considered the most stable species on the pathway starting from **100_3**.

Under dehydrated conditions, the species **100_4** is the most stable; however, it can easily rearrange in **100_3**, which appears as a reaction precursor state ($\Delta E = 17$ kJ mol^{-1}). From **100_3**, the metathesis reaction is easy, mainly because the formation of the metallacyclobutane is equilibrated at room temperature (from ΔG calculations), thereby allowing a reduced barrier for the cycloreversal step. The larger free energy reaction barrier for this **100_3** site at room temperature is 36 kJ mol^{-1}, which corresponds to the cycloreversal step. In the presence of water, the **100_1** species is formed where the preferred metallacyclobutane conformation is more stable than reactants by $\Delta G = 30$ kJ mol^{-1}; thus, the reactivity is significantly decreased. Water appears as a poison, requiring a thermal treatment to reactivate the catalyst. At moderately higher reaction temperatures, the "hydrated" Mo species also may exhibit an activity in metathesis, if it is still stable.

3.5. Ethene metathesis: Mo sites on (110) γ-alumina

We return to the Mo species stable under moderately hydrated conditions, **110_1** and **110_2**. The ethene-molybdenamethylidene complex **110_1ec** is the initial intermediate of ethene addition to the Mo-methylidene center **110_1** (Fig. 8). The ethene complex is slightly less stable than **100_3ec**, and its Mo–C_{ethene} and C–C distances are intermediate between the corresponding values for **100_1ec** and **100_3ec** (Figs. 5, 7, and 8). Conversion of **110_1ec** to the TBP molybdacyclobutane **110_1TBP** is almost barrierless and involves an energy gain of 20 kJ mol^{-1} (Fig. 8); however, analogous to the pathway for ethene metathesis on **100_1**, the subsequent SP molybdacyclobutane complex **110_1SP** can be readily formed. The transformation is exothermic by 44 kJ mol^{-1}, and the estimated Gibbs free energy relative to the reactants is -35 kJ mol^{-1} at room temperature. The metallacycle opening step is endothermic and activated (barrier 69 kJ mol^{-1}), thereby blocking the reaction; **110_1** is poorly active at room temperature. Again, the thermodynamic stability of **110_1SP** decreases with temperature, and $\Delta G = -19$ and 4 kJ mol^{-1} at 373 and 473 K, respectively.

The Mo-methylidene center **110_2** is predicted to be much more stable than the **110_1** one. Both TBP (**110_2TBP**) and SP (**110_2SP**) molybdacyclobutanes (Fig. 9) have been optimized as the potential intermediates of ethene metathesis proceeding on **110_2**; however, the calculated energy of ethene addition to this Mo site, leading to the TBP molybdacyclobutane, is highly endothermic ($\Delta E = 50$ kJ mol^{-1}; $\Delta G = 105$ kJ mol^{-1}). Therefore, on the basis of this result, we can conclude that the **110_2** site has a rather low activity (if any) in olefin metathesis.

The calculated relative energy of the SP molybdacyclobutane **110_2SP** ($\Delta E = -67$ kJ/mol) is not very different from the corresponding values reported earlier and is close to the results obtained with the cluster calculations [10,11]. The pre-

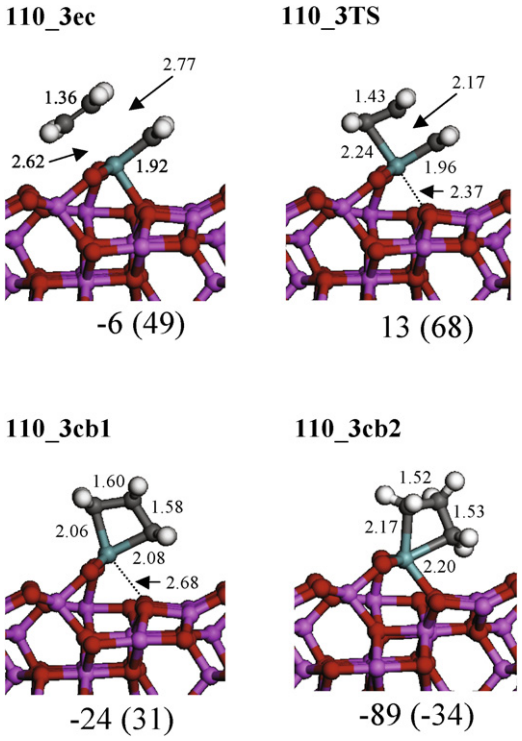

Fig. 10. Intermediates and transition states involved in ethene metathesis on the Mo-methylidene center **110_3**. The energies (kJ mol^{-1}) and Gibbs free energies (in parentheses, $T = 298$ K, kJ mol^{-1}), related to the reactants, are given below the structures.

dicted geometries of the molybdacyclobutane rings for the series **110_1** and **110_2** (Figs. 8 and 9) are similar to the corresponding molybdacyclobutane structures on the (100) surface of γ-alumina (Figs. 5–7).

In the case of ethene addition to the Mo-methylidene center **110_3**, the ethene-molybdenamethylidene complex **110_3ec** is a very shallow minimum on the potential energy surface, because its formation is exothermic by only 6 kJ mol^{-1} (Fig. 10). The conversion of the ethene complex to the molybdacyclobutane intermediate **110_3cb1** involves a low energy barrier (19 kJ mol^{-1}), which is, however, higher than for the aforementioned transition states. The predicted activation energy of the cycloreversal step (37 kJ mol^{-1}) is still moderate, but the rearrangement of **110_3cb1** to the much more stable conformer **110_3cb2** is more likely. The latter has a puckered ring, whereas the ring in the former is flat. Actually, **110_3cb1** is a transition state between two puckered conformers, symmetrical to each other, one of which is **110_3cb2**. The predicted energy and Gibbs free energy of the molybdacyclobutane **110_3b2**, relative to the initial Mo-methylidene center and ethene, are almost the same as for **110_1SP** (Fig. 8), again implying moderate catalytic activity.

Note that the bond between the molybdenum and the three-coordinated oxygen atom O4 (Figs. 3 and 10) is almost broken in the molybdacyclobutane **110_3cb1** (2.68 Å), in contrast to the Mo-methylidene center **110_3** and the second molybdacyclobutane **110_3cb2**, in which the Mo–O4 bond is recovered. The geometrical parameters of the rings in **110_3cb1** and **110_3cb2** (Fig. 10) are close to the corresponding values for the TBP and SP molybdacyclobutanes, respectively (Figs. 5–9).

The molybdacyclobutane complex **110_4cb** (Fig. 9), which has a trigonal bipyramidal geometry, is a potential intermediate involved in ethene metathesis proceeding on the Mo-methylidene center **110_4**. But its formation is predicted to be irreversible, because the calculated energy of ethene addition to the **110_4** is -115 kJ mol^{-1}, and the estimated Gibbs free energy is negative at temperatures as high as 473 K. Therefore, this center seems to be highly reactive toward alkenes, but rather poorly active (if at all) in alkene metathesis, at least at low temperatures. Although **110_4** has a geometry similar to that of **110_3**, the carbene bond in the former is much better exposed for the alkene attack. It was recently shown, based on cluster calculations, that the geometrical parameters of Mo-alkylidene sites influence their reactivity toward ethene [11]. The sum of the three angles that define the face where the alkene enters (here O2–Mo–C1 + O3–Mo–C1 + O2–Mo–O3; see Fig. 3) can be a convenient descriptor of the reactivity. The higher this sum, the better the exposure of the carbene bond toward alkene. Indeed, the sum of these angles is significantly larger for **110_4** (357°) than for **110_3** (336°), indicating the geometrical reasons for the differing activities.

The cycloaddition of ethene on the Mo-methylidene center **110_5** leads to the molybdacyclobutane intermediate **110_5cb1** with a flat ring (Fig. 11). Its formation is moderately exothermic and involves an energy barrier of 20 kJ mol^{-1}. The predicted activation energy for the splitting of **110_5cb1** to the Mo-methylidene + ethene is approximately 46 kJ mol^{-1}. As in most other cases, a second molybdacyclobutane structure with a puckered ring (**110_5cb2**) also has been localized, which can be in thermodynamic equilibrium with the reactants or products at room temperature. Its splitting to the Mo-methylidene + ethene through the isomeric structure **110_5cb1** requires at least 73 kJ mol^{-1} to pass the overall activation barrier. This possibility is not excluded at moderate and high temperatures, when the equilibrium is shifted toward Mo-methylidene + ethene.

Because the bond between the molybdenum and the two-coordinated surface oxygen O7 is broken in **110_5cb1** (compare **110_5**, Fig. 3, Table 3), the molybdenum is pentacoordinated, and the complex has a trigonal bipyramidal geometry. The Mo–O7 interaction is present again in the **110_5cb2** molybdacyclobutane (Fig. 11), where the molybdenum is hexacoordinated. The geometry of this complex can be described as a distorted pentagonal pyramid.

Note that the relative energies of **110_5cb1** and **110_5cb2** are quite close to those of **100_3TBP** and **100_3SP**, respectively (Figs. 7 and 11). But although the thermodynamics of the reaction are similar in both cases, the energy barrier is significantly higher for **110_5**, and an ethene complex is not formed here. This difference in activity can be discussed in terms of steric hindrance during the initial interaction between ethene and the Mo center. Again using the sum of the three angles mentioned earlier (here O1–Mo–C1 + O2–Mo–C1 + O1–Mo–O2; Figs. 1 and 3), this parameter is 338° for **100_3** and 317° for **110_5**. Therefore, the higher activity of the former can be explained by an easier access of ethene to the carbene bond.

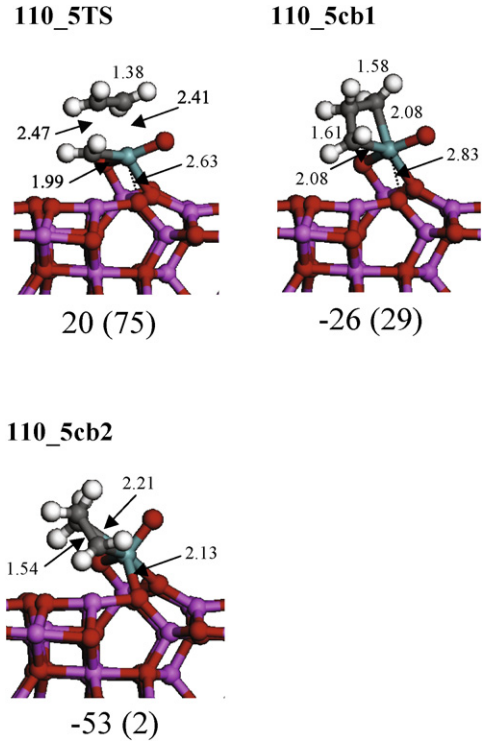

Fig. 11. Intermediates and transition states involved in ethene metathesis on the Mo-methylidene center **110_5**. The energies (kJ mol^{-1}) and Gibbs free energies (in parentheses, $T = 298$ K, kJ mol^{-1}), related to the reactants, are given below the structures.

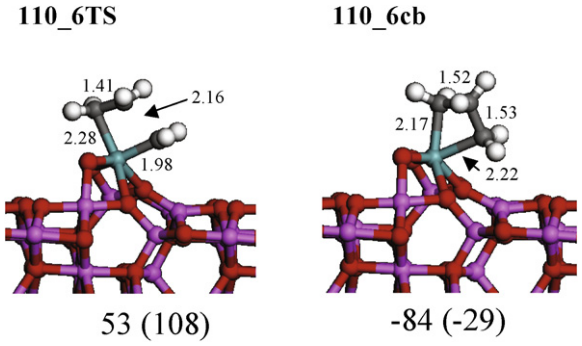

Fig. 12. The transition state and molybdacyclobutane complex involved in ethene metathesis on the Mo-methylidene center **110_6**. The energies (kJ mol^{-1}) and Gibbs free energies (in parentheses, $T = 298$ K, kJ mol^{-1}), related to the reactants, are given below the structures.

Moreover, breaking of the single Mo–O bond in **110_5TS** and **110_5cb1** (Fig. 11) also can contribute to the higher activation barrier.

The surface complex **110_6cb** (Fig. 12) is the only molybdacyclobutane structure localized as the potential intermediate of ethene metathesis on the Mo-methylidene **110_6** (Fig. 3). The molybdenum in **110_6cb** is hexacoordinated, and the Mo–C and C–C distances are similar to the corresponding bond lengths in the SP molybdacyclobutanes (Figs. 5–9). The formation of **110_6cb** is irreversible at room temperature, and the predicted activation energy of this step is 53 kJ mol^{-1}. The cycloreversal step involves a much higher activation barrier of 137 kJ mol^{-1}. Therefore, **110_6**, which is the most stable Mo-methylidene center among the "dehydrated" species on the (110) surface, can be active in olefin metathesis only at high temperatures.

Table 6
Energy barriers ($\Delta E_1^{\ddagger}$ and $\Delta E_2^{\ddagger}$, kJ mol^{-1}; see Scheme 3) and Gibbs free energy barriers ($\Delta G_1^{\ddagger}$ and $\Delta G_2^{\ddagger}$, kJ mol^{-1}, $T = 298$ K; see Scheme 4) for the cycloaddition and cycloreversion steps, respectively, during ethene metathesis proceeding on the potentially active Mo-methylidene centers. In each case the most stable metallacycle is considered. Structures **100_2**, **110_2** and **110_4** are discarded because poorly active. **100_4** is a precursor of **100_3**

Site	$\Delta E_1^{\ddagger}$	$\Delta E_2^{\ddagger}$	$\Delta G_1^{\ddagger}$	$\Delta G_2^{\ddagger}$
100_1	11	84	54	84
100_3	5	36 (46[a])	30	36 (46[a])
110_1	5	69	34	69
110_3	19	102	68	102
110_5	20	73	75	73
110_6	53	137	108	137

[a] The formation of **100_4cb** is assumed.

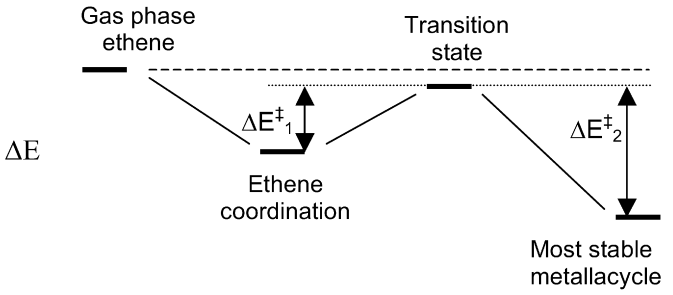

Scheme 3.

3.6. Metathesis activity of the Mo sites: A summary

The metathesis activity of the Mo-methylidene species on γ-alumina strongly depends on their geometries and locations. This statement is consistent with the results of previous theoretical studies based on the cluster approximation [10,11]. On the other hand, obtaining some relevant structures in which the molybdenum is three- or four-fold bonded to the surface was not possible using those finite cluster models. The current periodic DFT calculations, based on more reliable models of the γ-alumina surface, provide comprehensive information on the metathesis active sites on the molybdena-alumina system.

According to the present calculations, the Mo-methylidene species on the (100) surface of γ-alumina can be active at room temperature if they are dehydrated (**100_3** structure). On the other hand, the Mo centers on (110) γ-alumina are rather poorly active, but they are stable complexes. Table 6 summarizes the calculated activation barriers for ethene metathesis. The definitions of the activation parameters are explained in Schemes 3 and 4. As shown, **100_3** is the best candidate for the metathesis active site at room temperature. The most stable "dehydrated" Mo species on the (110) face (**110_6**) can be active only at high temperatures, whereas the most active species on this surface are **110_1** and **110_5**. But the latter is less stable than **110_6** by 42 kJ mol^{-1}, and the poorly active "hydrated" species **110_2** is much more stable than **110_1** (by 71 kJ mol^{-1}).

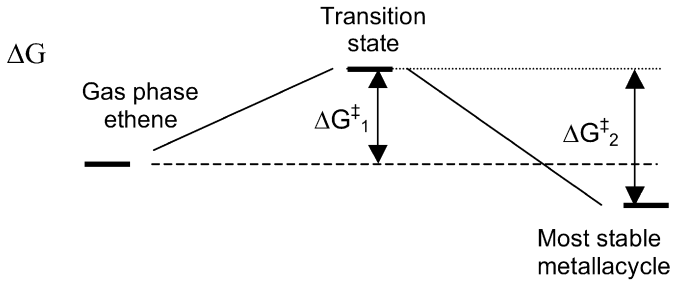

Scheme 4.

The reported apparent activation energies of propene metathesis on molybdena-alumina catalysts are in the range of 7–37 kJ mol^{-1} [14–16,51]. A true activation energy of 34 kJ mol^{-1} was derived from experimental kinetic data, applying the Langmuir–Hinshelwood model [52]. This value is close to the activation barrier predicted for ethene metathesis on the Mo-methylidene **100_3** sites (Table 6), whereas the other sites studied involve much higher barriers, due mainly to the easy formation of the more stable molybdacyclobutane form. According to our results, the stable molybdacyclobutane forms are in thermodynamic equilibrium with the reactants/products at room temperature (**100_3SP**, **110_5cb2**) or at higher temperatures (**100_1SP**, **110_1SP**, **110_3cb2**, **110_6cb**). Therefore, a significant part of the potentially active Mo sites are present during metathesis reaction in the form of the stable molybdacyclobutane species, a low energy point in the potential energy surface, thereby blocking the reactivity of a large fraction of sites. Only two Mo species (**100_3** and **110_5**) exhibit thermoneutral molybdacyclobutane formation. Among these, only **100_3** shows a low barrier and is active at room temperature; it can be readily formed from the most stable **100_4** species on this surface. (This formation requires only 17 kJ mol^{-1}.) This species is in low concentration for two reasons: The (100) surface is a minority face on γ-alumina particles, and the grafted complexes on this termination are less stable than that on the majority (110) surface. This predicted small number of catalytically active sites is fully consistent with their very low concentration determined experimentally for molybdena-alumina systems (<1% of the total Mo atoms) [28]. Moreover, the **100_4** site is stable only under dehydrated conditions, and thus traces of water should destroy the catalytic activity.

4. Conclusions

We have used a periodic slab model for the first time to investigate ethene metathesis on molybdena-alumina catalyst through a periodic DFT approach. We modeled numerous potential monomeric Mo-methylidene centers located differently on the (100) and (110) surfaces of γ-alumina. In these structures, the molybdenum is twofold-, threefold-, or fourfold-bonded to the surface. According to our DFT calculations and thermodynamic analysis, the relative stabilities of different Mo-methylidene species depend on temperature and water vapor pressure. We also can predict that the Mo sites on the (110) surface are more stable than their analogues located on the (100) face.

We examined the activity of the Mo-methylidene centers by investigating the pathways for ethene metathesis. Our calculations show a large range of reactivity toward alkenes for the considered Mo sites on both the (100) and (110) surfaces of γ-alumina. The metathesis activity of the Mo-methylidene centers depends strongly on their geometries and locations on the γ-alumina surface. Most Mo-methylidene centers are reactive with ethene and form the molybdacyclobutane species.

The energy of the formation of two key molybdacyclobutane intermediates from Mo-methylidene and ethene are decisive factors in the efficiency of a given Mo site in the metathesis reaction. The first molybdacyclobutane species is formed directly after the addition of ethene to the carbene bond, and its splitting to Mo-methylidene + ethene would be a continuation of the catalytic cycle of ethene metathesis; however, isomerization of the first molybdacyclobutane to a second, more stable structure is more likely. This step can be considered a reversible deactivation route, because the cycloreversal can proceed only via the first molybdacyclobutane intermediate.

In many cases, the molybdacyclobutane species are significantly more stable than the reactants. Thus, metallacycle opening to restore carbene and olefin is the rate-limiting step in olefin metathesis. The large majority of sites, although reactive with ethene, are blocked at the molybdacyclobutane step, with low catalytic reactivity at room temperature. Among the 10 grafted complex structures studied, only **100_3** and its precursor **100_4** are catalytically active at room temperature. The role of the alumina solid support, compared with a coordination complex, is to impose a constraint on the Al–O–Mo bonds, thereby deforming the Mo environment. The reduced stability of the metallacycle on the **100_3** site, and hence its high catalytic activity, are related to the large deformation imposed by the surface on the coordination of the Mo atom.

Water acts as a poison for the molybdena-alumina catalyst because, among other possible effects caused by moisture, the hydrated sites are less catalytically active. The most active Mo-methylidene center (**100_3 or 100_4**) is stable on the (100) surface only under dehydrated conditions. This surface is a minority termination for γ-alumina particles (17%). Moreover, the grafted Mo complexes are less stable on this termination than on the (110) surface. Thus, the proportion of such sites should be very low. At higher temperatures, however, other Mo species on both γ-alumina faces can exhibit activity in olefin metathesis.

In this work, we have studied 10 potential Mo-methylidene centers on the two alumina surfaces that predominate on alumina particles. These structures are proposed to be representative of the types of sites present on the catalyst. In real catalysts, various surface irregularities could be present, which would increase the number of possibilities; thus, we do not claim to have described the exact structure of the active site. Our key finding is that the various Mo species show strikingly different activities, as a function of the constraints imposed on the complex by the grafting site. Therefore, only a small fraction of the Mo sites are very active. Better chemical control of the grafting process is needed to produce "single-site" catalysts with higher activity.

Thus, our DFT calculations provide insight into the structure of surface active sites, their relative stability and reactivity, and the role of the substrate to constraint the surface species.

Acknowledgments

This work was performed under project HPC-EUROPA (RII3-CT-2003-506079), with the support of the European Community-Research Infrastructure Action under the FP6 "Structuring the European Research Area" Programme. Computing resources from Institut du Développement et des Ressources en Informatique Scientifique (IDRIS) and Academic Computer Center CYFRONET AGH (grants MEiN/SGI3700/PK/021/2006 and MNiSW/SGI4700/PK/044/2007) are gratefully acknowledged.

References

[1] J.C. Mol, J. Mol. Catal. A 213 (2004) 39.
[2] J.L.G. Fierro, J.C. Mol, in: J.L.G. Fierro (Ed.), Metal Oxides: Chemistry and Applications, Taylor & Francis, Boca Raton, FL, 2006, p. 517.
[3] E. Folga, T. Ziegler, Organometallics 12 (1993) 325.
[4] Y.-D. Wu, Z.-H. Peng, J. Am. Chem. Soc. 119 (1997) 8043.
[5] Y.-D. Wu, Z.-H. Peng, Inorg. Chim. Acta 345 (2003) 241.
[6] L. Cavallo, J. Am. Chem. Soc. 124 (2002) 8965.
[7] S.F. Vyboishchikov, M. Bühl, W. Thiel, Chem. Eur. J. 8 (2002) 3962.
[8] C. Adlhart, P. Chen, Angew. Chem. Int. Ed. 41 (2002) 4484.
[9] T.P.M. Goumans, A.W. Ehlers, K. Lammertsma, Organometallics 24 (2005) 3200.
[10] J. Handzlik, J. Ogonowski, R. Tokarz-Sobieraj, Catal. Today 101 (2005) 163.
[11] J. Handzlik, Surf. Sci. 601 (2007) 2054.
[12] J.-L. Hérisson, Y. Chauvin, Makromol. Chem. 141 (1971) 161.
[13] K.A. Vikulov, I.V. Elev, B.N. Shelimov, V.B. Kazansky, J. Mol. Catal. 55 (1989) 126.
[14] W. Grünert, A.Yu. Stakheev, R. Feldhaus, K. Anders, E.S. Shpiro, Kh.M. Minachev, J. Catal. 135 (1992) 287.
[15] W. Yi, M. Schwidder, W. Grünert, Catal. Lett. 86 (2003) 113.
[16] Y. Iwasawa, H. Kubo, H. Hamamura, J. Mol. Catal. 28 (1985) 191.
[17] M. Anpo, M. Kondo, Y. Kubokawa, C. Louis, M. Che, J. Chem. Soc. Faraday Trans. 1 84 (1988) 2771.
[18] T. Ono, M. Anpo, Y. Kubokawa, J. Phys. Chem. 90 (1986) 4780.
[19] H. Hu, I.E. Wachs, S.R. Bare, J. Phys. Chem. 99 (1995) 10897.
[20] G. Xiong, C. Li, Z. Feng, P. Ying, Q. Xin, J. Liu, J. Catal. 186 (1999) 234.
[21] R. Radhakrishnan, C. Reed, S.T. Oyama, M. Seman, J.N. Kondo, K. Domen, Y. Ohminami, K. Asakura, J. Phys. Chem. B 105 (2001) 8519.
[22] C. Li, J. Catal. 216 (2003) 203.
[23] A.N. Desikan, L. Huang, S.T. Oyama, J. Chem. Soc. Faraday Trans. 88 (1992) 3357.
[24] M.A. Vuurman, I.E. Wachs, J. Phys. Chem. 96 (1992) 5008.
[25] D.S. Kim, I.E. Wachs, K. Segawa, J. Catal. 146 (1994) 268.
[26] G. Mestl, T.K.K. Srinivasan, Catal. Rev. Sci. Eng. 40 (1998) 451.
[27] I.E. Wachs, in: J.L.G. Fierro (Ed.), Metal Oxides: Chemistry and Applications, Taylor & Francis, Boca Raton, FL, 2006, p. 1.
[28] J. Handzlik, J. Ogonowski, Catal. Lett. 88 (2003) 119.
[29] G.C. Bazan, E. Khosravi, R.R. Schrock, W.J. Feast, V.C. Gibson, M.B. O'Regan, J.K. Thomas, W.M. Davis, J. Am. Chem. Soc. 112 (1990) 8378.
[30] G.C. Bazan, J.H. Oskam, H.-N. Cho, L.Y. Park, R.R. Schrock, J. Am. Chem. Soc. 113 (1991) 6899.
[31] R.R. Schrock, in: A. Fürstner (Ed.), Topics in Organometallic Chemistry. Alkene Metathesis in Organic Synthesis, vol. 1, Springer, Berlin, 1998, p. 1.
[32] R.R. Schrock, A.H. Hoveyda, Angew. Chem. Int. Ed. 42 (2003) 4592.
[33] A. Hu, K.M. Neyman, M. Staufer, T. Belling, B.C. Gates, N. Rösch, J. Am. Chem. Soc. 121 (1999) 4522.
[34] A. Goursot, B. Coq, F. Fajula, J. Catal. 216 (2003) 324.
[35] M. Digne, P. Sautet, P. Raybaud, P. Euzen, H. Toulhoat, J. Catal. 211 (2002) 1.
[36] M. Digne, P. Sautet, P. Raybaud, P. Euzen, H. Toulhoat, J. Catal. 226 (2004) 54.
[37] J. Joubert, P. Fleurat-Lessard, F. Delbecq, P. Sautet, J. Phys. Chem. B 110 (2006) 7392.
[38] J. Joubert, A. Salameh, V. Krakoviack, F. Delbecq, P. Sautet, C. Copéret, J.M. Basset, J. Phys. Chem. 110 (2006) 23944.
[39] G. Kresse, J. Hafner, Phys. Rev. B 47 (1993) 558.
[40] G. Kresse, J. Furthmüller, Comput. Mater. Sci. 6 (1996) 15.
[41] G. Kresse, J. Furthmüller, Phys. Rev. B 54 (1996) 11169.
[42] J.P. Perdew, J.A. Chevary, S.H. Vosko, K.A. Jackson, M.R. Pederson, D.J. Singh, C. Fiolhais, Phys. Rev. B 46 (1992) 6671.
[43] G. Kresse, D. Joubert, Phys. Rev. B 59 (1999) 1758.
[44] G. Mills, H. Jónsson, G.K. Schenter, Surf. Sci. 324 (1995) 305.
[45] H. Jónsson, G. Mills, K.W. Jacobsen, in: B.J. Berne, G. Ciccotti, D.F. Coker (Eds.), Classical and Quantum Dynamics in Condensed Phase Simulations, World Scientific, Singapore, 1998, p. 385.
[46] X. Krokidis, P. Raybaud, A.-E. Gobichon, B. Rebours, P. Euzen, H. Toulhoat, J. Phys. Chem. B 105 (2001) 5121.
[47] H. Knözinger, P. Ratnasamy, Catal. Rev. Sci. Eng. 17 (1978) 31.
[48] L.J. Alvarez, J.F. Sanz, M.J. Capitán, M.A. Centeno, J.A. Odriozola, J. Chem. Soc. Faraday Trans. 89 (1993) 3623.
[49] R. Tokarz-Sobieraj, K. Hermann, M. Witko, A. Blume, G. Mestl, R. Schlögl, Surf. Sci. 489 (2001) 107.
[50] J. Joubert, F. Delbecq, P. Sautet, E. Le Roux, M. Taoufik, C. Thieuleux, F. Blanc, C. Copéret, J. Thivolle-Cazat, J.-M. Basset, J. Am. Chem. Soc. 128 (2006) 9157.
[51] E.S. Davie, D.A. Whan, C. Kemball, J. Catal. 24 (1972) 272.
[52] A.J. Moffat, A. Clark, J. Catal. 17 (1970) 264.